In dark analysis of PVA/AA materials at very low spatial frequencies: phase modulation evolution and diffusion estimation

Sergi Gallego[1,*], Andrés Márquez[1], Stephan Marini[1], Elena Fernández[2], Manuel Ortuño[1], Inmaculada Pascual[2]

[1]*Dept. Física Enginyeria de Sistemes i Teoria del Senyal, Universitat d'Alacant (Spain) Apartat 99 E-03080 Alacant*
[2]*Dept. Òptica, Farmacologia i Anatomia, Universitat d'Alacant (Spain) Apartat 99 E-03080 Alacant*
**Sergi.Gallego@ua.es*

Abstract: Molecular diffusion effects have been widely studied inside photopolymers for holographic applications. Recently some works have focused on low spatial frequencies to evaluate in real time the monomer diffusion effects. Assuming a Fermi-Dirac function-based profile, we have fitted the diffracted intensities, reflected and transmitted (up to the 8th order), to obtain the phase and surface profile of the recorded gratings. We have studied the influence of diffusion in polyvinyl-alcohol/acrylamide for the range of spatial frequencies between 2 lines/mm and 6 lines/mm. We have demonstrated the influence of the spatial frequency on the magnitude and sign of the material volume variations. We also studied in dark the evolution of the grating shape. We show that it is possible to achieve diffractive gratings with diffraction efficiency in the first order near 35% if the in dark evolution is taken into account. Furthermore we present a method to calculate the monomer diffusivity in photopolymers. The differential equation is deduced and solved, and experimental average value is obtained (D=1.1·10^{-8} cm^{2}s^{-1}).

OCIS codes: (160.5470) Polymers; (290.1990) Diffusion, (09.0090) Holography

References and links

1. A. Pu, and D. Psaltis, "High-density recording in photopolymer-based holographic three-dimensional disks," Appl. Opt. **35**(14), 2389–2398 (1996).
2. Y. Tomita, K. Furushima, K. Ochi, K. Ishizu, A. Tanaka, M. Ozawa, M. Hidaka, and K. Chikama, "Organic nanoparticle (hyperbranched polymer)-dispersed photopolymers for volume holographic storage," Appl. Phys. Lett. **88**(7), 071103 (2006).
3. Márquez, C. Neipp, S. Gallego, M. Ortuño, A. Beléndez and I. Pascual, "Edge enhanced imaging using PVA/acrylamide photopolymer gratings," Opt. Lett. **28**, 1510–1512 (2003).
4. V. Weiss, E. Millul, and A. A. Friesem, "Improvements in holographic photopolymers at Weizmann Institute of Science," SPIE International Technical Group Newsletter: Optics in Information Systems **15**(1), 3 (2004).
5. J. V. Kelly, M. R. Gleeson, C. E. Close, F. T. O' Neill, J. T. Sheridan, S. Gallego, and C. Neipp, "Temporal analysis of grating formation in photopolymer using the nonlocal polymerization-driven diffusion model," Opt. Express **13**, 6990–7004 (2005).
6. S. Gallego, C. Neipp, M. Ortuño, A. Beléndez, E. Fernández, and I. Pascual, "Analysis of diffusion in depth in photopolymer materials," Opt. Commun. **274**(1), 43–49 (2007).
7. K. Pavani, I. Naydenova, S. Martin, and V. Toal, "Photoinduced surface relief studies in an acrylamide-based photopolymer," J. Opt. A, Pure Appl. Opt. **9**(1), 43–48 (2007).
8. A. Márquez, J. Campos, M. J. Yzuel, I. Pascual, A. Fimia, and A. Beléndez, "Production of computer-generated phase holograms using graphic devices: application to correlation filters," Opt. Eng. **39**(6), 1612–1619 (2000).
9. S. Gallego, A. Márquez, D. Méndez, S. Marini, A. Beléndez, and I. Pascual, "Spatial phase modulation-based study of PVA/AA photopolymers in the low spatial frequency range," Appl. Opt. **48**, 4403–4413 (2009).
10. A. Márquez, C. Iemmi, I. Moreno, J. A. Davis, J. Campos, and M. J. Yzuel, "Quantitative prediction of the modulation behavior of twisted nematic liquid crystal displays," Opt. Eng. **40**(11), 2558–2564 (2001).
11. S. Gallego, A. Márquez, D. Méndez, C. Neipp, M. Ortuño, M. L. Alvarez, E. Fernandez, A. Beléndez, and I. Pascual, "Real-time interferometric characterization of a polyvinyl alcohol based photopolymer at the zero spatial frequency limit," Appl. Opt. **46**(30), 7506–7512 (2007).

#114022 - $15.00 USD Received 8 Jul 2009; revised 18 Aug 2009; accepted 2 Sep 2009; published 25 Sep 2009

12. S. Gallego, A. Márquez, D. Méndez, M. Ortuño, C. Neipp, M. L. Alvarez, A. Beléndez, E. Fernández, and I. Pascual, "Analysis of PVA/AA based photopolymers at the zero spatial frequency limit using interferometric methods," Appl. Opt. **47**(14), 2557–2563 (2008).
13. S. Gallego, A. Márquez, D. Méndez, C. Neipp, M. Ortuño, A. Beléndez, E. Fernández, and I. Pascual, "Direct analysis of monomer diffusion times in polyvinyl/acrylamide materials," Appl. Phys. Lett. **92**(7), 073306 (2008).
14. T. Endo, F. Sanda, "Ring-opening polymerization, anionic (with expansion in volume)," Polymeric Materials Encyclopedia, **10**, CRC Press, Inc.,7550–3, (1996).
15. G. Ramos, A. Álvarez-Herrero, T. Belenguer, F. del Monte, and D. Levy, "Shrinkage control in a photopolymerizable hybrid solgel material for holographic recording," Appl. Opt. **43**(20), 4018–4024 (2004).
16. L. Dhar, M. G. Schones, T. L. Wysocki, H. Bair, M. Schilling, and C. Boyd, "Temperature-induced changes in photopolymer volume holograms," Appl. Phys. Lett. **73**(10), 1337–1339 (1998).
17. I. Naydenova, E. Mihaylova, S. Martin, and V. Toal, "Holographic patterning of acrylamide-based photopolymer surface," Opt. Express **13**(13), 4878–4889 (2005).
18. T. Babeva, I. Naydenova, S. Martin, and V. Toal, "Method for characterization of diffusion properties of photopolymerisable systems," Opt. Express **16**(12), 8487–8497 (2008).
19. V. Moreau, Y. Renotte, and Y. Lion, "Characterization of dupont photopolymer: determination of kinetic parameters in a diffusion model," Appl. Opt. **41**(17), 3427–3435 (2002).
20. F. T. O'Neill, J. R. Lawrence, and J. T. Sheridan, "Improvement of holographic recording material using aerosol sealant," J. Opt. **3**, 20–25 (2001).

1. Introduction

Photopolymer properties, such as high diffraction efficiencies, low noise, self-developing, easy preparation, high thickness, low cost, etc., make these optical recording materials optimum media for many applications [1–3]. Photopolymer formulations contain a dye, a cosensitizer, one or two monomers and a binder. In general, the diffusion velocity depends on the particular photopolymer composition. Nevertheless, the binder is the more important factor to determine the diffusion of the components inside the material. In polyvinyl-alcohol/acrylamide (PVA/AA) based materials PVA is used as a binder and the quantity of water that remains in the layer depends on the molecular weight and the drying process [4]. On the other hand the presence of triethanolamine (TEA) as a cosensitizer changes the diffusion properties (TEA is a liquid at ambient temperature). The influence of species diffusion in the phase image formation in photopolymers has been analyzed by many authors [5–7]. Some models of hologram formation based on the diffusion and polymerization processes are used to determine values of monomer diffusivity. One of the problems associated to this method, used for the holographic cases, is the very short diffusion times obtained for high spatial frequencies. Therefore, for spatial frequencies around 1000 lines/mm, the species diffusion only can be determined indirectly. In this work to observe in real time the effects of species diffusion, we record very low spatial frequency elements. We store low spatial frequency gratings and we evaluate the material behavior after recording process. We focus our attention in two aspects: the in dark evolution of the grating phase-modulation shape and the volume changes in the material surface. Assuming a Fermi-Dirac function-based profile, we have fitted the diffracted intensities, reflected and transmitted (up to the 8th order), to obtain the phase and surface profile of the recorded gratings [8,9]. We have evaluated three different spatial frequencies between 2 lines/mm and 6 lines/mm. We have chosen this range of spatial frequency since diffusion effects after recording take place after a few seconds of the recording process start. The method to store gratings is based on a dynamic experimental set up where a spatial phase modulator (SLM) is working in amplitude only configuration [10], determines the spatial frequency. This work is based on previous works where we analyzed the lowest spatial frequency [11,12], the zero spatial frequency limit, and some low spatial frequencies [13].

2. Experimental

2.1 Fitted Profile

The Fermi-Dirac based profile is a better option [9] than the super-Gaussian based profile used in previous works [8], due mainly to two reasons: the parameters in the Fermi-Dirac function are continuous whereas in the super-Gaussian function the parameter describing the sharpness of the edges is discrete, thus there is no gradual transition between the fitted

#114022 - $15.00 USD Received 8 Jul 2009; revised 18 Aug 2009; accepted 2 Sep 2009; published 25 Sep 2009

profiles; furthermore, the Fermi-Dirac function provides a very good fit to the cosine function, which may be considered as a reasonable limit case when edges become highly smoothed by diffusion. The mathematical expression for the amplitude transmission $t(x)$ of a transparent phase element showing a Fermi-Dirac phase profile $\varphi(x)$ can be written as follows,

$$t(x) = \exp\left(i\varphi(x)\right) \tag{1}$$

$$\varphi(x) = \varphi_0\left(1+\exp\left(\alpha\cdot\left(\frac{|x|}{\Omega}-1\right)\right)\right)^{-1} \tag{2}$$

where φ_0 is the asymptotic phase modulation depth (for an x-interval (-∞,+∞)), Ω controls the symmetry (or duty cycle) of the profile, and α is the parameter characterizing the function shape and sharpness of the edges. The function is limited to an x-interval (–1,1), and repeated periodically. We consider symmetric gratings, that for this x-interval correspond to a value of Ω=0.5. We rescale the phase values obtained in the x-interval (–1,1) so that the phase modulation depth in this finite interval equals the asymptotic phase modulation depth.

We have compared the diffraction efficiencies calculated numerically using the Fermi-Dirac model with the experimental values for the first 9 orders (orders from 0 to 8).

2.2. Experimental set-up

The experimental set-up is shown in Fig. 1. We have used an expanded, collimated recording beam provided by a solid-state Verdi laser (Nd-YVO4) with a wavelength of 532 nm (at this wavelength the dye exhibits a maximum absorption). The exposure intensity is 0.5 mW/cm^2. The periodic pattern is introduced by a liquid crystal display (LCD), a Sony LCD model LCX012BL, extracted from a video projector Sony VPL-V500. We use the electronics of the video projector to send the voltage to the pixels of the LCD. The LCD is used in the amplitude-mostly modulation regime by proper orientation of the external polarizers (P) [10]; then the pattern is imaged onto the material with an increased spatial frequency (a demagnifying factor of 2). The use of the LCD allows us to change the period of the grating recorded in the photopolymer without moving any mechanical part of the set-up. To analyze in real time the variation in efficiency of the different diffraction orders, we use an unexpanded beam of a He-Ne laser (633 nm) incident at a small angle with respect to the normal axis of the recording material. A diaphragm (stop2) is placed in the focal plane of the relay lens so as to eliminate the diffraction orders produced by the pixelation of the LCD. In this work the patterns sent to the LCD correspond to binary gratings with different periods. It can be expected that the final pattern imaged onto the recording material will be low filtered due to the finite aperture of the imaging system and especially due to the filtering process produced by stop2.

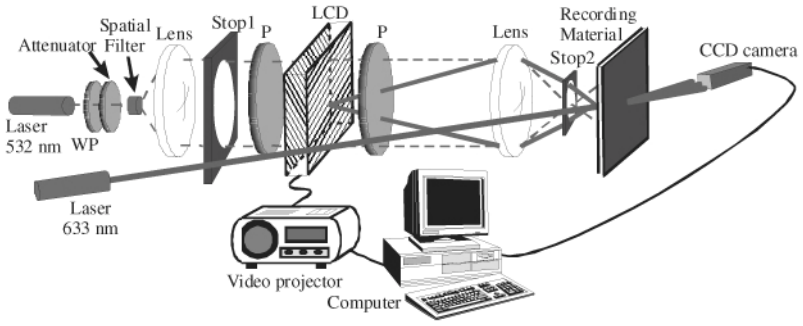

Fig. 1. - Experimental set-up used to analyze the recording of gratings in real time.

#114022 - $15.00 USD Received 8 Jul 2009; revised 18 Aug 2009; accepted 2 Sep 2009; published 25 Sep 2009

To obtain the Fourier transform of the pattern and then to measure the diffracted intensities (of transmitted and reflected orders), we may place a lens after the grating (recorded in the photopolymer). The Fourier plane is captured using a CCD camera at the focal plane of the lens. We use the CCD camera model pco.1600 from pco.imaging. This is a high dynamic 14 bits cooled CCD camera system with a resolution of 1600x1200 pixels, and a pixel size of 7.4x7.4 μm^2. The high dynamic range together with the high number of pixels allows us to use this camera as a radiometer where the intensity directed to the various diffraction orders (in our case 9 orders) can be measured in parallel. We have estimated experimentally the error of the diffraction efficiencies obtained using this camera and it turns out to be around 0.5%.

The photopolymers used to store the gratings are similar to the ones used in previous works [10–12]. In this sense the material preparation is similar to the one presented in the previous work [9]. The PVA/AA formulations contain a dye (yellowish eosin), a cosensitizer which is triethanolamine (TEA), two monomers (AA with N,N'-methylenebisacrylamide) and a polymer as a binder (PVA). The final "dried" layers used in the recording step have a thickness of 90±5μm.

3.- Results and discussion

In this section, we have evaluated the evolution of the gratings after the recording process, i.e. the in dark evolution. We have focused our attention in two important factors: the shape of the edges of the phase-modulation profile and the diffraction efficiencies of the first diffracted order (high values of first diffracted order are required for its application to fabricate diffractive optical elements [8,9]). Firstly, we have analyzed the phase gratings stored measuring the diffracted orders. Studying these data, we have fitted the phase shape of the grating. The phase modulation is due to the refractive index modulation and the thickness changes. Furthermore to have a deeper insight into the volume variations we have measured the reflected orders, and have obtained the profile surface shape after the exposition. We have used these data together with a simple model based on the Fick's law to calculate the average species diffusivity inside the material.

3.1. Transmission analysis

As we have noted in the introduction, we have analyzed the material behavior in a range of spatial frequencies where species diffusion begins to play an important role in the phase image formation [9]. In this sense, the lowest spatial frequency corresponds to a period of 0.672 mm. We have exposed the layer to the recording pattern during 200 s and then we have analyzed the changes in the grating using red illumination. The intensities of the 4th first orders are depicted in Fig. 2(a), the initial behavior is similar than the presented in ref [9]. As we can see orders 0 and 2 present variations during relax period. On the other hand, the order 3 remains constant around 13% of diffraction efficiency. Taking into account the 8 first orders we have fitted the shape profiles in three different times, during recording, when the recording stops and 200 s later. The results are presented in Fig. 2(b). It is possible to see the smoothing of the edges during recording and the light variations during non-exposure stage. Nevertheless it can be seen the poor influence of diffusion in very low spatial frequencies on the phase depth.

#114022 - $15.00 USD Received 8 Jul 2009; revised 18 Aug 2009; accepted 2 Sep 2009; published 25 Sep 2009

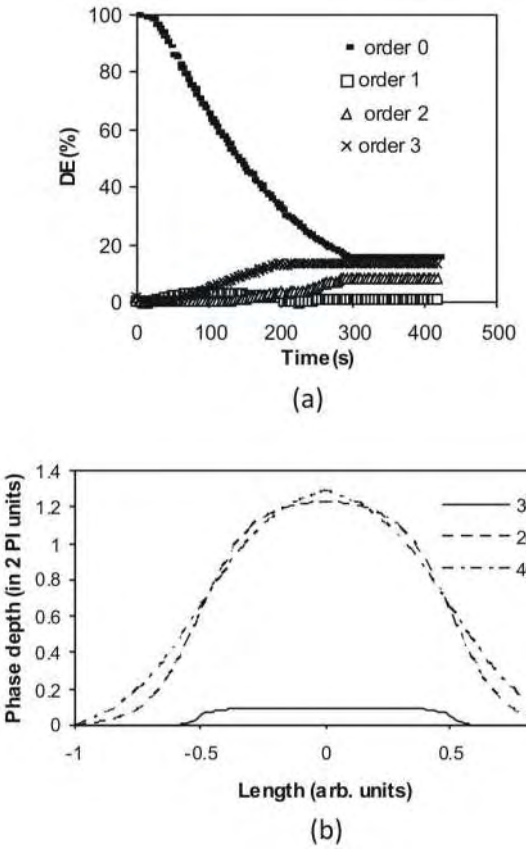

Fig. 2. - Gratings with a spatial period of 0.672 mm in transmission case. (a) Diffraction intensities of the first 4 orders. (b) Estimated profiles for different times (at 30 s of exposure time, when exposure stops at 200 s, and 200 s later).

To understand when diffusion becomes important, we have recorded gratings with a spatial period of 0.336 mm. In Fig. 3, we have represented the evolution of the 4 main diffracted orders when the recording stops at 200 s. To analyze the evolution in the stored phase profiles, we have sketched the shape for three different times. We have also checked if there exists smoothing of the gratings period and if the phase modulation decreases due to species diffusion. It is important to compare the profiles obtained after 200 s (just when exposition stops) and after 400 s (200 s after the end of exposition). As it can be seen there exists an important decrease of the phase depth (Fig. 3(b)). This phenomenon can be explained by the transport of material from the dark zones to the bright ones due to species diffusion. In this sense, it is important to remark that we have detected the swelling of the bright zones. This effect will be analyzed more accurately in the next section. Therefore, we can conclude that when spatial periods of 0.336 mm are recorded effects of species diffusion cannot be disregarded, since species diffusion become very relevant in the phase image formation processes. It is important to note the chance to obtain high values of the first diffracted order for this spatial frequency when exposition stops at 16 s. In Fig. 3(c) the values of the first order become constant around 35% of diffraction efficiency.

#114022 - $15.00 USD Received 8 Jul 2009; revised 18 Aug 2009; accepted 2 Sep 2009; published 25 Sep 2009

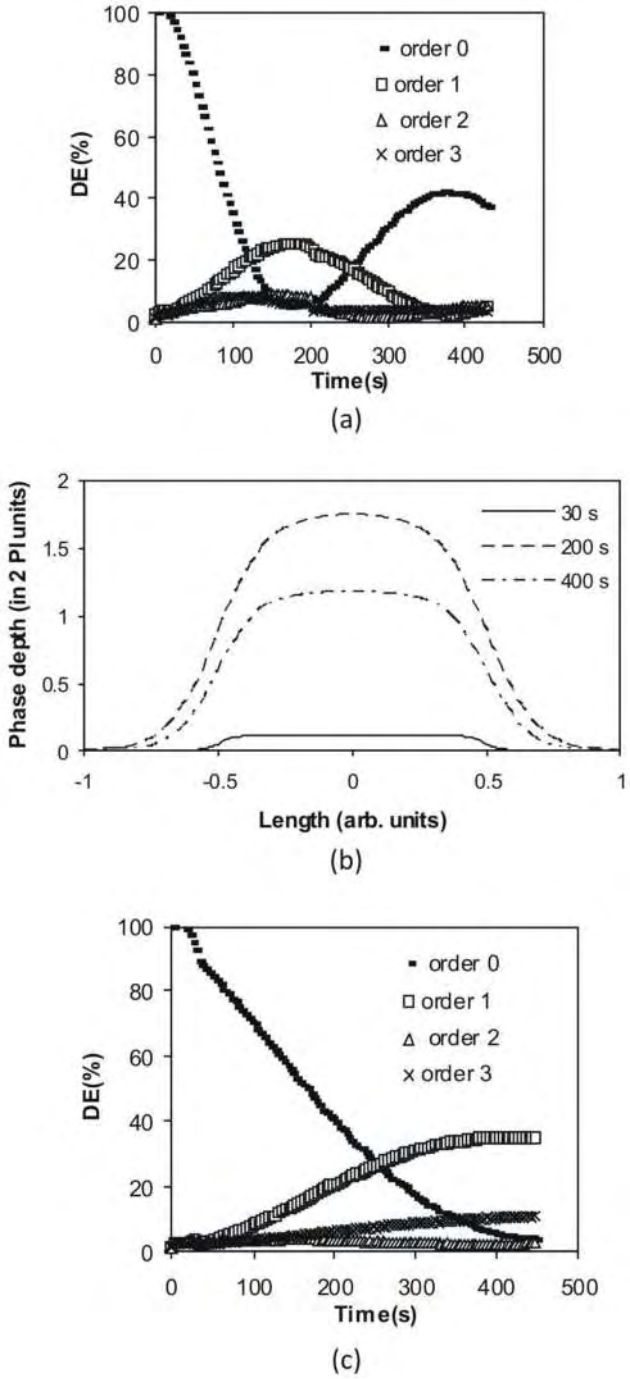

Fig. 3. - Gratings with a spatial period of 0.336 mm analyzed for transmission case. (a) Diffraction intensities of the first 4 orders when exposure stops after 200 s. (b) Estimated profiles for different times. (c) Diffraction intensities of the first 4 orders when exposition stops after 16 s.

When gratings with a spatial period of 0.168 mm are exposed the effects of species diffusion can be observed in real time too. The intensities of the different diffraction orders change after exposition and the effects of species diffusion are comparable to the

#114022 - $15.00 USD Received 8 Jul 2009; revised 18 Aug 2009; accepted 2 Sep 2009; published 25 Sep 2009

polymerization. In order to produce a diffractive optical element with prescribed diffraction efficiencies we can calculate the time when exposure should stop, as we can predict what the evolution due to diffusion will be. To analyze the importance of this phenomenon we have followed the same experimental procedure: the analysis of the stored profile. In Figs. 4(a) and 4(b) we can see a clear smoothing of the edges due to species diffusion. We can also note how the 35% of phase modulation is lost 200 s after exposition finishes (Fig. 4(b)). Now it is important to know which part of decreasing is due to the volume variation. This information can be obtained through an analysis of the reflected orders as we show in the next section. At this point, it is important to estimate the percentage of the phase decrease due to volume variations of the material.

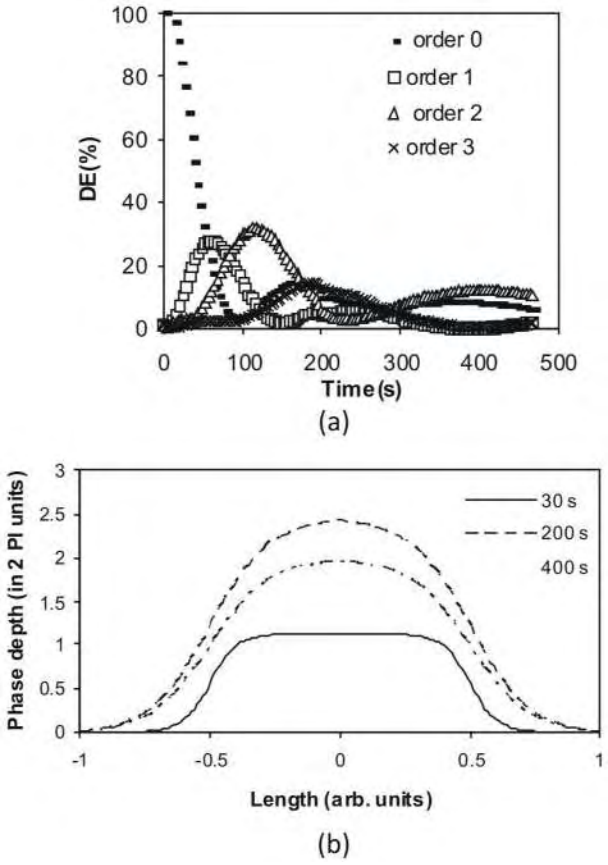

Fig. 4. - Gratings with a spatial period of 0.168 mm in the transmission case. (a) Diffraction intensities of the first 4 orders. (b) Estimated profiles for different exposition times. Exposition stops at 200 s.

3.2 Reflection analysis

In this section we will evaluate the volume variation during and after exposure by measuring the reflected diffracted orders. In order to eliminate the secondary reflection we introduce a black PVC adhesive on the second glass surface. As we already noted in previous papers [12], phase modulation is higher than 20π for long exposures. At this point of our analysis, we must take into account that our technique based on measuring the diffraction efficiencies of the different diffraction orders presents some difficulties for high values of phase depth [9]. The sum of the diffraction efficiencies for the first 9 orders (0 to 8) decreases to values lower than a 10% in just 200 s. In this case we already explained in reference 9 that these low values were due to the large phase modulation depths exhibited by the surface profile and basically

#114022 - $15.00 USD Received 8 Jul 2009; revised 18 Aug 2009; accepted 2 Sep 2009; published 25 Sep 2009

for α values smaller than 5 (i.e. smoothed profiles). These weak values of the first 9 orders produce a large uncertainty in the fitting of the profile. In particular, we observed that the values obtained for the α parameter looked reasonable, providing the expected smoothed profile, but the phase depths φ_0 obtained were even much larger than expected. In fact, we can say that we have an ambiguity in the phase depth since there is a set of different φ_0 values giving a very similar fit; these values are practically equal modulus 2π. To solve this problem we stop the recording only after 16 s of exposition. In this case the phase depth is around 2π [12], and so we can obtain the surface profile using de Fermi-Dirac function without ambiguities.

In Fig. 5(a), it is possible to see clear and important variations in the diffracted intensities due to species diffusion. The figure represents the relaxing process of a grating with spatial period of 0.672 mm when the exposition stops after 16 s. The shape grating evolution is depicted in Fig. 5(b), where the smoothing of the edges is clearly appreciated; we can also see the decreasing of the shrinkage due to species diffusion from the dark zones to bright ones. This variation is small due to the size of the spatial period analyzed. To observe the effects of the species diffusion clearly, we studied surface gratings with a spatial period of 0.168 mm.

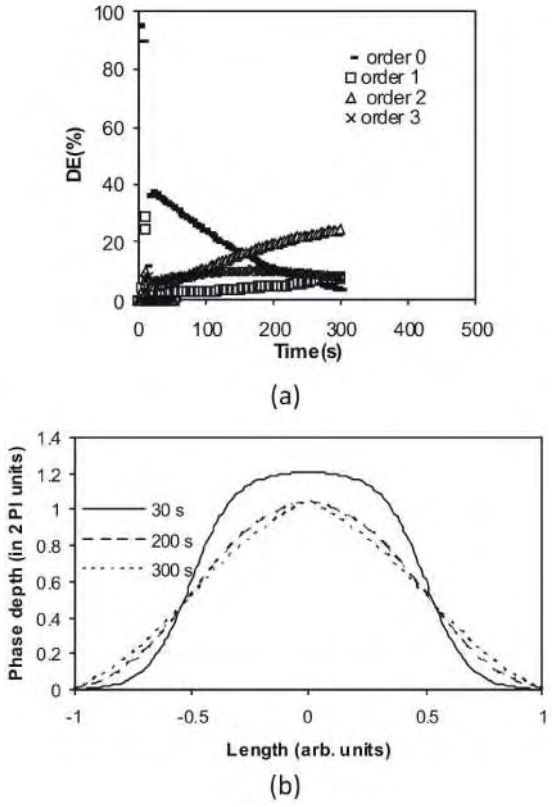

Fig. 5. - Gratings a with spatial period of 0.672 mm in the reflection case. (a) Diffraction intensities of the first 4 orders. (b) Estimated profiles for different exposure times. Exposition stops at 16 s.

Shrinkage and swelling in photopolymers have been discussed by many authors [14–18]. It is well known that shrinkage occurs when monomer molecules begin to link forming chains of polymer, compacting the layer and decreasing the holes size. On the other hand, the monomer and dye diffusion from the dark zones to bright ones (where they are consumed) contributes to the swelling. At very high spatial frequencies, it is difficult to prove the swelling and only the average shrinkage of the illuminated area can be measured. At lower spatial frequencies using the grating analysis we can determine accurately the importance of

#114022 - $15.00 USD Received 8 Jul 2009; revised 18 Aug 2009; accepted 2 Sep 2009; published 25 Sep 2009

diffusion in surface volume changes. To obtain a deep insight into the influence of species diffusion on the surface relief we have analyzed the grating profile evolution for gratings with a period of 0.168 mm. The grating was exposed during just 16 s. We have evaluated the changes in the surface grating when the exposition stops. In Fig. 6(a), we represent the variation of the diffractive efficiencies of the 4 first orders during and after exposition. As can be seen when exposition finishes, at 16 s, the diffracted energy is concentrated in 0 order (90%), and the higher orders are weak (less than 4%). To analyze the phenomenon that generates this behavior we have evaluated the evolution of the refractive index. In Fig. 6(b), we present the profiles for six different exposition times. Firstly, we have obtained the profile when the recording is stopped (after 16 seconds), the phase depth is around 2π. Afterwards the phase depth starts to decrease and after 90 s the surface grating is very weak (according to the process followed in ref [12], 0.2π radians phase depth corresponds to thickness amplitude of 20 nm), in other words, the volume differences between bright and non illuminated areas have reduced due to the species diffusion inside the material. Later, the depth of the grating begins to grow again due to the material addition from the dark zones to the illuminated ones. At this point we have measured the swelling of the illuminated areas as mentioned by Babeva et al. [18]. The exact time when shrinkage disappears depends on the exposition time and on the spatial frequency recorded. This important fact must be taken into account in the models of image formation in photopolymers.

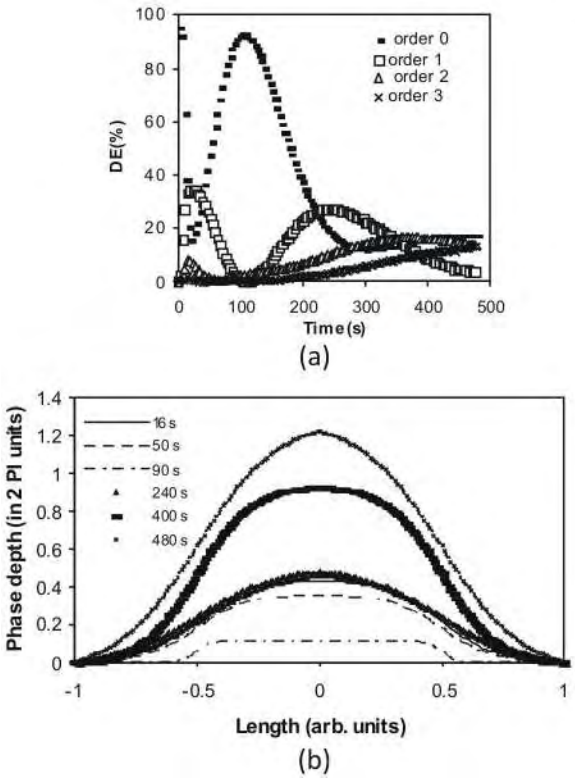

Fig. 6. - Gratings with spatial period of 0.168 mm in the reflection case. (a) Diffraction intensities of the first 4 orders. (b) Estimated profiles for different exposition times. Exposition stops at 16 s (we give the absolute value for phase depth).

3.3 Diffusion estimation

From the analysis about the grating surface evolution after exposure carried out in the last section, we have obtained qualitative and quantitative information about species diffusion inside the material. Recent work [18] has proposed one simple method to calculate diffusion

#114022 - $15.00 USD Received 8 Jul 2009; revised 18 Aug 2009; accepted 2 Sep 2009; published 25 Sep 2009

values based on Fick's law [19] recording only one single spot. The study consists in the variation of the profile shape for different spot sizes (the diameter of the spots are around 50 μm). The temporal variation of monomer concentration ($m(x,t)$) is expressed as a function of the spatial variations of monomer diffusion ($D(x,t)$) and monomer concentration and can be written as:

$$\frac{\partial m(x,t)}{\partial t} = \frac{\partial}{\partial x}\left[D(x,t)\frac{\partial m(x,t)}{\partial x} \right] \tag{3}$$

During the short exposition process there exists shrinkage due to the polymerization. Once exposition stops, in reference [18] the height of the profile, (*h*), is proportional to the monomer concentration. In the case presented in our work we have a periodic structure and few hours after the exposure, when the monomer is again uniformly distributed we have the polymer underlying profile. Therefore in our experiments $h(x,t)$ is given as:

$$h(x,t) = V_m\, m\ (x,t) + V_p\, p(x) \tag{4}$$

Where V_m is the molar volume of monomer and V_p is the molar volume of polymer and *p(x)* is the polymer concentration. Therefore the measured volume variations, $\Delta h(x,t)$, observed in the grating profile after expositions can be written as:

$$\Delta h(x,t) = h(x,t) - h_0(x) = V_m\,(m_0(x,t) - m_0(x)) \tag{5}$$

Where $m_0(x)$ and $p(x)$ are the monomer and polymer concentrations when illumination stops (time independent) and in the first attempt unknown. In other words, after exposition, the *h* variations are proportional to the monomer variations.

In this sense, to solve the Fick's law (Eq. (3)) after a periodic illumination we have proposed the following model. Due to the exposition a monomer concentration distribution is generated inside the photopolymer ($m(x,t)$). Exponential decay (increase) of monomer concentration in the non-exposed (exposed) zones due to monomer diffusion (as we have depicted in Fig. 7) begins when the exposition stops to achieve the average value of the residual monomer (m_f) , corresponding to the point when the monomer diffusion eventually stops due to uniform monomer distribution.

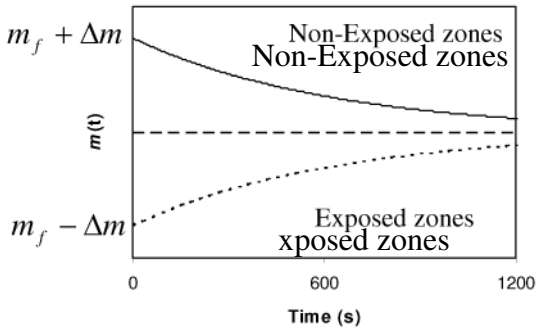

Fig. 7. Variation of amplitude of monomer concentration as a function of time after exposure in the exposed zones and non-exposed ones.

In this sense we can describe the monomer concentration as:

$$m(x,t) = m_f + \Delta m(x)\exp\left(\frac{-t}{\tau}\right) \tag{6}$$

#114022 - $15.00 USD Received 8 Jul 2009; revised 18 Aug 2009; accepted 2 Sep 2009; published 25 Sep 2009

where the monomer modulation is $\Delta m(x)$ and τ is the characteristic time of monomer variation and can be calculated by fitting the *h* variation with time [13,20]. When we introduce this expression in Eq. (3) we obtain:

$$\Delta m(x) = -\tau \frac{\partial}{\partial x}\left[D(x,t) \frac{d\Delta m(x)}{dx} \right] \tag{7}$$

In a first approximation we can assume a sinusoidal distribution of the modulation of monomer concentration and for the illumination (*I*):

$$\Delta m(x) = \Delta m_0 \cos\left(\frac{2\pi x}{\Lambda} \right) \tag{8}$$

$$I(x) = I_0 \left(1 - \cos\left(\frac{2\pi x}{\Lambda} \right) \right) \tag{9}$$

where Λ is the grating period. This assumption makes sense just for very short exposures and sinusoidal distribution of the recording intensity. Therefore the Eq. (7) can be rewritten as:

$$tg\left(\frac{2\pi}{\Lambda} \right) \frac{\partial}{\partial x} D(x,t) + \frac{2\pi}{\Lambda} D(x,t) - \frac{\Lambda}{2\pi\tau} = 0 \tag{10}$$

We obtain a first order differential equation, inhomogeneous, with constant coefficients, therefore the general solution is:

$$D(x) = \frac{\Lambda^2}{4\pi^2 \tau} + D_1 \csc\left(\frac{2\pi}{\Lambda} x \right) \tag{11}$$

It is important to note the simplicity of the Eq. (11), only two parameters determine the value of *D*: *Λ* and τ. In the case analyzed in this section the exposition time is 16 s and the exposure intensity is 0.5 mW/cm^2. Therefore polymer concentration is small and we can assume that *D* is spatially independent.

$$D = \frac{\Lambda^2}{4\pi^2 \tau} \tag{12}$$

In our analysis about the evolution of *h* in time, we have noted that the profile modulation, Δ*h,* achieved becomes time independent, after a time range of hours to few days after exposition. The approximation to this value is exponential. Next we show how we can obtain the value for the parameter τ, needed in Eq. (12), from the fitting of the temporal variation for Δ*h.* If we combine Eq. (5) and (6) we obtain:

$$\Delta h(x,t) = V_m \Delta m(x) \left(\exp\left(\frac{-t}{\tau} \right) - 1 \right) \tag{13}$$

This value tends asymptotically (in practice in a few hours) to the value:

$$\Delta h(x, t \to \infty) = -V_m \Delta m(x) \tag{14}$$

Thus, Eq. (13) can be rewritten as:

$$\Delta h(x, t \to \infty) - \Delta h(x,t) = \Delta h(x, t \to \infty) \exp\left(-t / \tau \right) \tag{15}$$

If we apply the logarithm to the both sides of the expression, we obtain:

#114022 - $15.00 USD Received 8 Jul 2009; revised 18 Aug 2009; accepted 2 Sep 2009; published 25 Sep 2009

$$\ln\left(\Delta h(x,t\to\infty)-\Delta h(x,t)\right)=\ln\left(\Delta h(x,t\to\infty)\right)-t/\tau \qquad (16)$$

We note that to derive Eq. (16) we have not assumed any specific profile for $\Delta m(x)$. To analyze the relation between h and phase depth, it is important to note that the variation in the phase depth when exposure stops is due to the species diffusion from the dark zones to bright ones. The movement of monomer from the dark zones to bright ones creates shrinkage in the dark zones and swelling in the bright ones.

In order to determine the value of τ and Δh, we have fit the experimental values obtained from Fig. 6 (one grating recording during 16 seconds). We have applied this Eq. (16) at x=0, where illumination takes the maximum value. We have studied the evolution of the diffraction efficiency during 9 days in order to estimate an accurate value of the limit of $\Delta h(t\to\infty)$. It is important to remark that in our case, this limit is different to zero in opposition to the data related in other experiments using PVA/AA based materials [18]. In Fig. 8 we represent the fitting used to calculate τ. The value of R^2 represented in this figure shows the agreement between the experiments and the theoretical behaviour assumed. Using the data from Fig. 8 we obtain the following values: $\tau = 625\,s$ and $D = 1.1\cdot 10^{-8}\,cm^2 s^{-1}$ this value agrees with the values of reference [13].

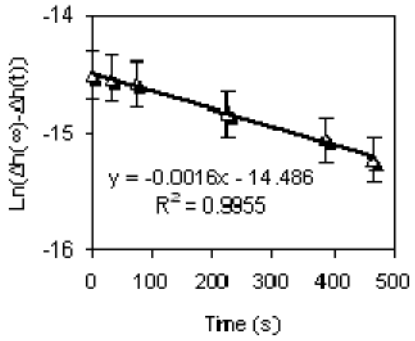

Fig. 8. - Logarithm of variation of h as a function of time for a grating with a spatial period of 0.168 mm.

The results obtained show that this method is a direct and efficient method to characterize diffusion properties in photopolymerisable systems. It is interesting to note that the obtained value of D in reference [18] is quite large, which explains why the spots disappear after 300 s. Maybe this difference is due to the different composition and the laboratory conditions during dried process.

Conclusions

Based upon experimental data and novel theoretical simulations (analyzing the material behaviour during in dark evolution) a thorough analysis of PVA/AA materials is presented. We have analyzed different spatial frequencies both measured in transmission and in reflection. This work allows us to eliminate many assumptions so as to obtain the species diffusivity inside the material. Furthermore if the diffusion phenomena are well predicted, it is possible to achieve diffractive gratings with very high values of diffraction efficiency in the first order (near 35%). We have checked that surface relieves remain stable several weeks after the recording process. This is an important preliminary step to build diffractive elements with stable properties with PVA/AA photopolymers. On the last place we have proposed a new method to model and measure the average monomer diffusivity in photopolymers. The value obtained for the PVA/AA photopolymer used in this work is $D = 1.1\cdot 10^{-8}\,cm^2 s^{-1}$.

#114022 - $15.00 USD Received 8 Jul 2009; revised 18 Aug 2009; accepted 2 Sep 2009; published 25 Sep 2009

Acknowledgements

This work was supported by the "Ministerio de Edicación y Ciencia" (Spain) under projects FIS2008-05856-C02-01 and FIS2008-05856-C02-02, by the Generalitat Valenciana (projects ACOMP/2009/150 and ACOMP/2009/160) and by Generalitat Valenciana under project GVPRE/2008/137.

#114022 - $15.00 USD Received 8 Jul 2009; revised 18 Aug 2009; accepted 2 Sep 2009; published 25 Sep 2009